Measurement of Separated Structure Functions in the $p(e,e'p)\pi^0$ Reaction at Threshold and Chiral Perturbation Theory

M. O. Distler,[1] A. M. Bernstein,[4] K. I. Blomqvist,[1] W. U. Boeglin,[1] R. Böhm,[1] R. Edelhoff,[1] J. Friedrich,[1] R. Geiges,[1] M. Kahrau,[1] M. Korn,[1] H. Kramer,[1] K. W. Krygier,[1] V. Kunde,[1] M. Kuss,[2] A. Liesenfeld,[1] H. Merkel,[1] K. Merle,[1] R. Neuhausen,[1] Th. Pospischil,[1] M. Potokar,[3] A. Rokavec,[3] A. W. Richter,[1] G. Rosner,[1] P. Sauer,[1] St. Schardt,[1] H. Schmieden,[1] S. Širca,[3] B. Vodenik,[3] A. Wagner,[1] Th. Walcher,[1] and St. Wolf[1]

[1]*Institut für Kernphysik, Universität Mainz, D-55099 Mainz, Germany*
[2]*Institut für Kernphysik, TH Darmstadt, D-64289 Darmstadt, Germany*
[3]*Institute "Jožef Stefan", University of Ljubljana, SI-1001 Ljubljana, Slovenia*
[4]*Massachusetts Institute of Technology, Cambridge, Massachusetts 02139*
(Received 10 November 1997; revised manuscript received 21 November 1997)

The reaction $p(e,e'p)\pi^0$ has been studied very close to threshold $\Delta W \leq 4$ MeV and at 4-momentum transfer $Q^2 = 0.1$ (GeV/c)^2. The scattered electron and the kinematically focused recoil proton were detected in coincidence using the 3-magnetic spectrometer setup at the Mainz Microtron MAMI. The transverse and longitudinal as well as the longitudinal-transverse and the transverse-transverse interference structure functions have been determined. From the data the s-wave multipoles E_{0+} and L_{0+} have been extracted. The experimental results are compared to recent calculations in chiral perturbation theory. [S0031-9007(98)05554-9]

PACS numbers: 13.60.Le, 12.39.Fe, 25.30.Rw

The pion is the lightest hadron and plays a decisive role in the structure of the nucleon. It is understood as a "Goldstone boson" reflecting the spontaneous symmetry breaking of the QCD vacuum. At low energies, where the color confinement makes the hadrons the only observable degrees of freedom, the Goldstone bosons provide a connection to QCD. Since the interaction of the light mass Goldstone bosons is weak at low energies, effective field theories can be formulated and observables can be calculated perturbatively in a momentum and quark mass expansion. This approach to low energy QCD is called "chiral perturbation theory" (ChPTh). It comprises two aspects which make an experimental verification interesting. In the first place, the intricate calculations of one- and two-pion-loop corrections and the range of validity of the renormalization of ChPTh requiring counter terms with constants not given in the framework of ChPTh have to be checked. Second, if from such a study a consistent picture emerges, the dynamic consequences of spontaneous symmetry breaking in QCD can be quantified.

The foundation was laid by Weinberg (see [1] and references therein) and originally limited to systems containing only pions. Consecutively ChPTh was applied in detail to $\pi\pi$ [2] and πN [3] reactions. However, due to the well known electromagnetic interaction, the photo- and electroproduction of pions promise particularly significant tests of the limits of validity and permit the determination of the low energy constants. The respective theoretical investigations have been performed only recently [4]. It was the aim of the experiment described in this paper to show that pion electroproduction can achieve the accuracy to provide a meaningful test of ChPTh. Different theoretical approaches, e.g., in Ref. [5] are not discussed because of space limitations.

About 25 years ago, the reaction $e + p \rightarrow e' + p + \pi^0$ had been investigated experimentally at threshold and in the energy region of the $\Delta(1232)$ resonance [6–9]. But only total cross sections significantly above the pion production threshold and at relatively high 4-momentum transfers could be determined. The small cross sections close to threshold could not be measured at the old low duty cycle ($\leq$2%) electron accelerators, which also had a disturbing beam halo.

The advent of high current, high duty cycle accelerators after 1990, together with high resolution magnetic spectrometers, makes the low pion production cross sections at threshold and at low momentum transfer accessible in coincidence experiments. First such electroproduction experiments of neutral pions have been performed at NIKHEF with duty factors of 1% [10] and 30% [11]. The first experiment with an old generation accelerator had only limited accuracy. The latter experiment was focused on the energy range of the production threshold of charged pions to study possible isospin breaking effects. In the region significant for the ChPTh tests very close to threshold (invariant mass $W = 1073.24$ MeV, $\Delta W \leq 5$ MeV) this experiment had restricted precision.

This paper presents an investigation of the $p(e,e'p)\pi^0$ reaction very close to threshold at the Microtron MAMI, a 100%-duty-cycle-electron accelerator with 855 MeV electron energy [12] with an energy width of the beam at 120 keV (FWHM) and an absolute uncertainty of 100 keV. The beam current of 16 to 22 μA was measured with a Förster probe to a precision of $\pm$150 nA. The liquid hydrogen was circulated between a cylindrical target cell with a diameter of 2 cm and a heat exchanger by means of a fan. To further avoid local boiling, the beam has been wobbled over an area of 5×6 mm^2.

 0031-9007/98/80(11)/2294(4)$15.00

The beam position has been measured on an event by event basis to allow reconstruction of the reaction vertex and correction for energy loss. A luminosity of $1.1 \times 10^{37}\ \mathrm{cm}^{-2}\,\mathrm{s}^{-1}$ was reached in this way.

The experiment was performed using two of the three spectrometers A, B, and C of the A1-Collaboration [13]. The scattered electrons with B and the recoil protons with A were detected in coincidence. Despite the relatively small solid angles of magnetic spectrometers, complete coverage of the cm system was obtained close to threshold due to the "inverse kinematics" of the $p(e,e'p)\pi^0$ reaction. If ΔW is small the pion is almost at rest and the outgoing proton is ejected into a small cone around the 3-momentum transfer. The π^0 can be identified by calculating the missing mass from the 4-vectors of the incoming electron and the outgoing electron and proton. This idea was already used at DESY [8] and later with the mentioned experiments at NIKHEF [10,11]. A relatively high 4-momentum transfer of $Q^2 = 0.1\ (\mathrm{GeV}/c)^2$ was chosen. This allowed the usage of the 2 cm thick cylindrical target. It also facilitated the control of the spectrometers momentum and time-of-flight resolutions. On the other hand, early ChPTh calculations [14] were not applicable at this Q^2, but they were quickly extended [15] after the data of this experiment became available. The data were taken at fixed momentum transfer at three different incident electron energies of 435, 555, and 855 MeV in order to perform a transverse/longitudinal separation of the cross section. Figure 1 shows the kinematical parameters and Table I lists the chosen values. The recoil protons were identified in spectrometer A by their energy loss in the two successive scintillator layers in the focal plane. The remaining contamination by minimum ionizing particles π^+, μ^+, e^+ was less than 10^{-4}. About 20% of the true coincidences were triggered by negative pions produced in the target walls. They were rejected by a Čerenkov detector in spectrometer B.

The random background was reduced by appropriate cuts in the coincidence time spectra. After correcting the particles time of flight for their different orbit lengths in the spectrometer the coincidence time resolution was 1.1 ns (FWHM). The π^0s were identified by their missing mass peak at 135.0 MeV with an rms width of 1 MeV.

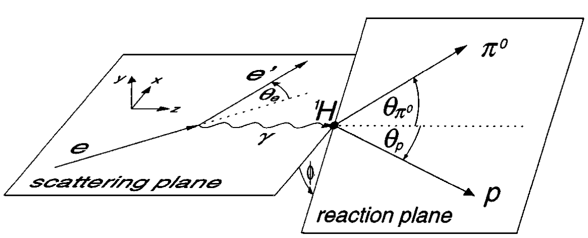

FIG. 1. The kinematical variables. The electron with momenta $\vec{e}$ and $\vec{e}'$ in the initial and final state, respectively, defines the scattering plane. The reaction plane defined by the pion π^0 and the proton p is tilted by an angle ϕ with respect to the scattering plane. The angle between the direction of the virtual photon γ and the neutral pion is denoted by θ_{π^0} and that for the proton by θ_p.

TABLE I. Kinematics in the laboratory frame. The central angles of the spectrometer for the electron θ_e and for the proton Θ_p are measured relative to the electron beam.

$Q^2 = 0.1\ (\mathrm{GeV}/c)^2, W = 1073.24$ MeV							
	ϵ	ϵ_L	E (MeV)	E' (MeV)	θ_e	$\lvert\vec{p}_p\rvert$ (MeV/c)	Θ_p
I	0.885	13.87	855	657	24.4°	326	46.6°
II	0.713	11.18	555	357	41.6°	326	39.5°
III	0.529	8.29	435	237	59.0°	326	33.0°

Finally, the resulting cross sections were corrected for radiation effects, detector inefficiencies, and dead-time loss. The acceptance was determined with a Monte Carlo simulation. The simulated distributions were checked with the uncorrelated single events and with measurements of elastic electron scattering on the proton. In both cases the simulation agreed with the data. The error of the absolute normalization was $\pm 1.5\%$ for the beam current and $\pm 1.7\%$ for the target thickness. A systematic error of $\pm 2\%$ for the radiative corrections was estimated. The largest contribution to the systematic error, however, arises from the uncertainty of the beam energy and of the momentum calibration of the electron spectrometer. This leads to a systematic uncertainty of the cross sections of 20% for the lowest energy bin at threshold and to 3% at 3.5 MeV above threshold.

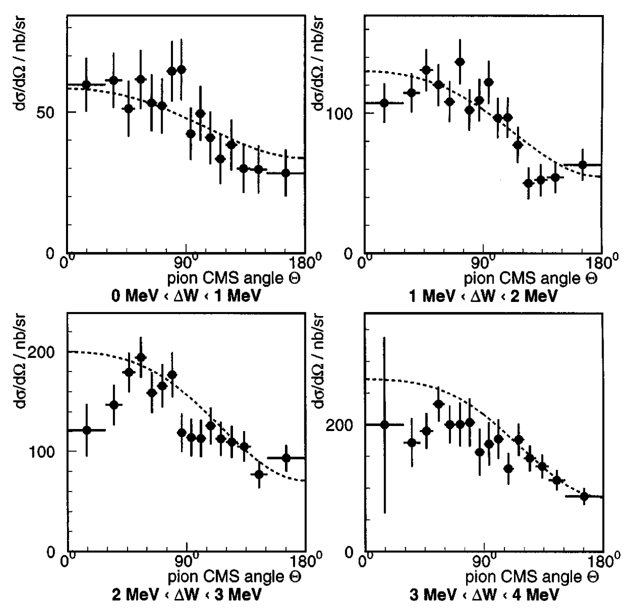

FIG. 2. The differential cross section $(d\sigma/d\Omega_\pi^*)$ as a function of the polar angle θ_π^* of the pion in the cm system at a beam energy of 555 MeV ($\epsilon = 0.713$) for four different regions in the invariant mass above production threshold. The dashed line shows the new fit of HBChPTh.

The coincidence cross section for pion electroproduction can be expressed as (see, e.g., [16])

$$\frac{d\sigma}{d\Omega_f d\epsilon_f d\Omega_\pi^*} = \Gamma\bigg(\frac{d\sigma_T}{d\Omega_\pi^*} + \epsilon_L \frac{d\sigma_L}{d\Omega_\pi^*} + \sqrt{2\epsilon_L(1+\epsilon)}\,\frac{d\sigma_{LT}}{d\Omega_\pi^*}\cos\phi_\pi^* + \epsilon\,\frac{d\sigma_{TT}}{d\Omega_\pi^*}\cos 2\phi_\pi^*\bigg), \quad (1)$$

where ϵ is the transverse polarization of the virtual photon and $\epsilon_L = (Q^2/\omega^{*2})\epsilon$. The pion angles ϕ_π^* and θ_π^* are the angles in the cm system corresponding to those in the laboratory frame illustrated in Fig. 1. The factor Γ is the flux of the virtual photon field. The first two terms of Eq. (1), the transverse (T) and longitudinal (L) cross sections, do not depend on the azimuthal angle. Therefore, they can be isolated by integrating over ϕ_π^*. Figure 2 shows $d\sigma/d\Omega_\pi^*$, i.e., the sum of the first two terms in Eq. (1), determined at 555 MeV. By using the different virtual photon polarizations the L and T cross sections were separated.

Because this measurement has complete kinematical coverage from threshold up to an invariant mass of 4 MeV above threshold, the dependence on the azimuthal angle can also be used to isolate the transverse-longitudinal (LT) and the transverse-transverse (TT) interference cross sections. Figures 3 and 4 show the experimental results. Taking all partial cross sections, the low energy constants of heavy baryon chiral perturbation theory (HBChPTh) in Ref. [15] have been newly fitted to the data of this experiment alone. The new values for the only two free parameters are $a_3 = -0.92 \pm 0.17$ and $a_4 = -0.99 \pm 0.13$ which has to be compared to the old values $a_3 = -1.46 \pm 0.14$ and $a_4 = -0.31 \pm 0.11$. It should be noted that the correlation between the two parameters is -0.99. The resulting curves are shown in Figs. 2–4.

Near threshold s- and p-wave amplitudes dominate the cross section [15,16] and the four parts of Eq. (1) can be written as

$$\begin{aligned}
\frac{d\sigma_T}{d\Omega_\pi^*} &= N\bigg\{|E_{0+}|^2 + \frac{1}{2}(|P_2|^2 + |P_3|^2) + 2\,\mathrm{Re}(E_{0+}P_1^*)\cos\theta_\pi^* + \Big[|P_1|^2 - \frac{1}{2}(|P_2|^2 + |P_3|^2)\Big]\cos^2\theta_\pi^*\bigg\},\\
\frac{d\sigma_L}{d\Omega_\pi^*} &= N[|L_{0+}|^2 + |P_5|^2 + 2\,\mathrm{Re}(L_{0+}P_4^*)\cos\theta_\pi^* + (|P_4|^2 - |P_5|^2)\cos^2\theta_\pi^*],\\
\frac{d\sigma_{LT}}{d\Omega_\pi^*} &= N[-\mathrm{Re}(E_{0+}P_5^* + L_{0+}P_2^*)\sin\theta_\pi^* + \mathrm{Re}(P_1P_5^* + P_4P_2^*)\sin\theta_\pi^*\cos\theta_\pi^*],\\
\frac{d\sigma_{TT}}{d\Omega_\pi^*} &= N\,\frac{1}{2}(|P_2|^2 - |P_3|^2)\sin^2\theta_\pi^*,
\end{aligned} \quad (2)$$

with q^* the pion cm momentum and $N = 2Wq^*/(W^2 - m_N^2)$. [In the notation $X_{l_\pi \pm (1/2)}$, X stands for the multipole character E (electric), L (longitudinal), M (magnetic), l_π denotes the angular momentum of the outgoing pion and the spin (1/2) of the nucleon is omitted.] The combinations of p-wave amplitudes P_i calculated with ChPTh are considered to be reliable because the one-pion-loop contributions are much smaller than those of the tree

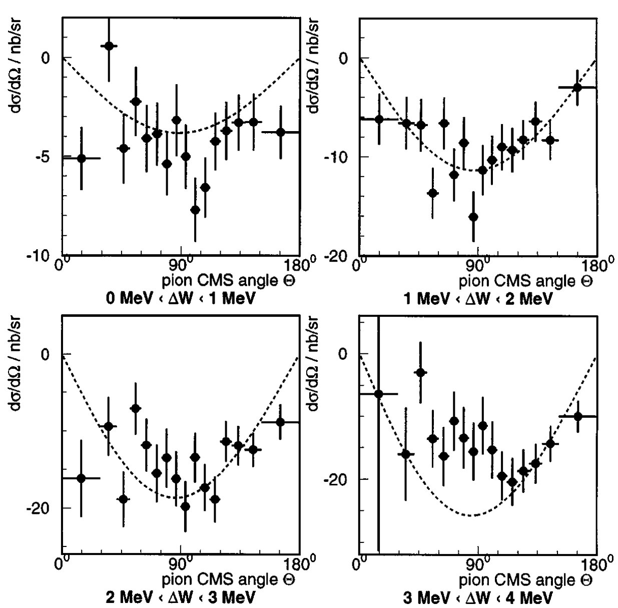

FIG. 3. The same as Fig. 2 for $d\sigma_{LT}/d\Omega_\pi^*$.

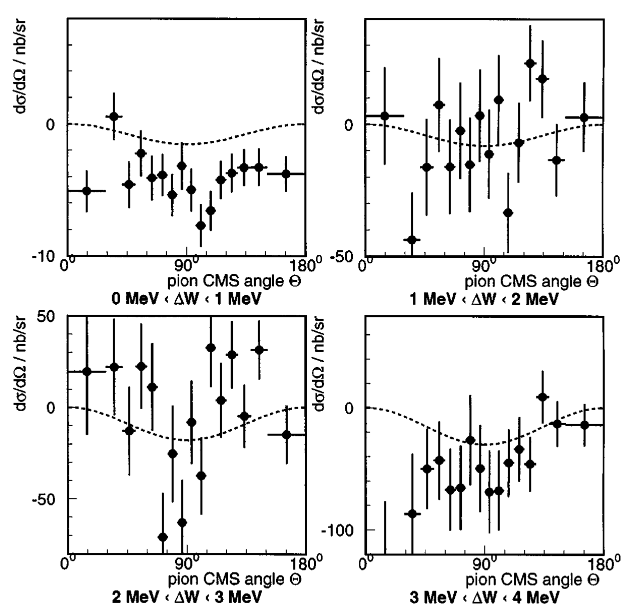

FIG. 4. The same as Fig. 2 for $d\sigma_{TT}/d\Omega_\pi^*$.

TABLE II. Results of the fit to the Mainz data. The upper rms error is statistical, the lower systematic.

$\Delta W/\text{MeV}$	0.5 ± 0.5	1.5 ± 0.5	2.5 ± 0.5	3.5 ± 0.5
$\frac{E_{0+}}{10^{-3}/m_\pi}$	$1.96^{\pm 0.33}_{\pm 0.29}$	$1.82^{\pm 0.19}_{\pm 0.19}$	$2.12^{\pm 0.17}_{\pm 0.20}$	$1.52^{\pm 0.18}_{\pm 0.16}$
$\frac{-L_{0+}}{10^{-3}/m_\pi}$	$1.42^{\pm 0.05}_{\pm 0.16}$	$1.41^{\pm 0.03}_{\pm 0.07}$	$1.36^{\pm 0.03}_{\pm 0.08}$	$1.27^{\pm 0.03}_{\pm 0.11}$
χ^2/n_f	1.29	1.19	1.68	1.84

diagrams. On the other hand, the s-wave amplitudes E_{0+} and L_{0+} need large one-pion-loop corrections even at $\Delta W = 0$ and $Q^2 = 0$, effectively destroying the classical low energy theorems. Therefore, using the predictions for the p-wave multipoles given in [15], Eq. (2) can be used to determine the s-wave multipoles E_{0+} and L_{0+}. Below the $\pi^+ n$ threshold ($\Delta W = 5.9$ MeV) all multipoles are real. $d\sigma_L/d\Omega_\pi^*$ and $d\sigma_T/d\Omega_\pi^*$ fix the values of L_{0+} and E_{0+} with the leading term. $d\sigma_{LT}/d\Omega_\pi^*$ represents an additional constraint [see Eq. (1)] in the common χ^2 fit of the s-wave amplitudes to the cross sections. The results are compiled in Table II and are depicted in Fig. 5 together with the NIKHEF results. The systematic error contains the mentioned uncertainty of the cross sections and a theoretical uncertainty of the $P_i s$ of $\pm 10\%$. It has to be noted that the NIKHEF results are derived without L/T separation and by using additional assumptions, e.g., that the imaginary part of the multipoles can be neglected.

The agreement between this experiment and the ChPTh fit is not bad, but it represents a test of limited significance only since theoretically undetermined parameters are fitted to the data. In order to avoid the need for the higher order constants and at the same time to make connection to the photo production at threshold [17–20], i.e., at $Q^2 = 0$, rather difficult experiments at $Q^2 < 0.1\ (\text{GeV}/c)^2$ have to be done. This work is in progress at MAMI. At the photon point $E_{0+} = (-1.31 \pm 0.08) \times 10^{-3} m_\pi$, i.e., is negative [18,20]. The experiment shows that the E_{0+} amplitude changes sign with increasing Q^2 and is predicted to be zero around $Q^2 = 0.04\ (\text{GeV}/c)^2$ [15].

In summary, the results of this study represent the first L/T separation and first determination of the LT and TT structure functions of the $p(e, e'p)\pi^0$ reaction close to threshold. The precision of the data is good enough to allow a meaningful confrontation with theory. However, a decisive test of ChPTh will need experiments at even lower Q^2.

This work was supported by the Deutsche Forschungsgemeinschaft.

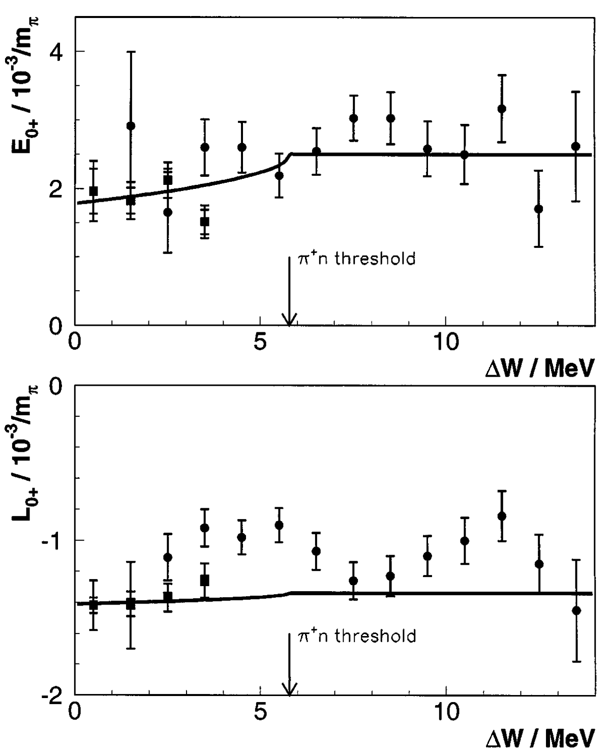

FIG. 5. The results for the real part of the amplitudes E_{0+} and L_{0+}. The small error bars of the Mainz data (■) represent the statistical, the wide bars the quadratic sum of the systematic and statistical error. The error bars of the NIKHEF data (●) are statistical only. The curves show the new fit of HBChPTh.

[1] S. Weinberg, Physica (Amsterdam) **96A**, 327 (1979).
[2] J. Gasser and H. Leutwyler, Ann. Phys. (N.Y.) **158**, 142 (1984).
[3] J. Gasser, M. E. Sainio, and A. Švarc, Nucl. Phys. **B307**, 779 (1988).
[4] For recent reviews, see G. Ecker, Prog. Nucl. Part. Phys. **35**, 1 (1995); V. Bernard, N. Kaiser, and U.-G. Meißner, Int. J. Mod. Phys. **E4**, 193 (1995).
[5] S. Scherer and J. H. Koch, Nucl. Phys. **A534**, 461 (1991).
[6] E. Amaldi *et al.*, Nuovo Cimento A **65**, 377 (1970).
[7] J. C. Alder *et al.*, Nucl. Phys. **B46**, 573 (1972).
[8] P. Brauel *et al.*, Phys. Lett. **50B**, 507 (1974).
[9] D. R. Botterrill *et al.*, Nucl. Phys. **116B**, 65 (1976).
[10] T. P. Welch *et al.*, Phys. Rev. Lett. **69**, 2761 (1992).
[11] H. B. van den Brink *et al.*, Phys. Rev. Lett. **74**, 3561 (1995); Nucl. Phys. **A612**, 391 (1997).
[12] J. Ahrens, H. Backe, D. von Harrach, K. H. Kaiser, F. Klein, R. Neuhausen, and Th. Walcher, Nucl. Phys. News **2**, 5 (1994).
[13] I. Blomqvist *et al.*, Nucl. Instrum. Methods Phys. Res. A **403**, 263 (1998).
[14] V. Bernard, N. Kaiser, T.-S. H. Lee, and U.-G. Meißner, Phys. Rep. **246**, 315 (1994).
[15] V. Bernard, N. Kaiser, and U.-G. Meißner, Nucl. Phys. **A607**, 379 (1996).
[16] D. Drechsel and L. Tiator, J. Phys. G **18**, 449 (1992).
[17] R. Beck *et al.*, Phys. Rev. Lett. **65**, 1841 (1990).
[18] M. Fuchs *et al.*, Phys. Lett. B **368**, 20 (1996); A. M. Bernstein *et al.*, Phys. Rev. C **55**, 1509 (1997).
[19] J. C. Bergstrom *et al.*, Phys. Rev. C **53**, 1052 (1996).
[20] J. C. Bergstrom *et al.*, Phys. Rev. C **55**, 2016 (1997).